Polarized Fluorescence Correlation Spectroscopy of DNA-DAPI Complexes

MARIA LUISA BARCELLONA,[1] SETH GAMMON,[2] THEODORE HAZLETT,[3] MICHELLE A. DIGMAN,[3] AND ENRICO GRATTON[3]

[1]*Department of Biological Chemistry and Molecular Biology, University of Catania, Catania, Italy 95125*
[2]*Mallinckrodt Institute of Radiology, Washington University, St. Louis, Missouri 63130*
[3]*Laboratory for Fluorescence Dynamics, Department of Physics, University of Illinois at Urbana-Champaign, Champaign, Illinois 61801*

KEY WORDS fluorescence correlation spectroscopy; rotational diffusion; 2-photon microscopy; anisotropy decay

ABSTRACT We discuss the use of fluorescence correlation spectroscopy for the measurement of relatively slow rotations of large macromolecules in solution or attached to other macromolecular structures. We present simulations and experimental results to illustrate the range of rotational correlation times and diffusion times that the technique can analyze. In particular, we examine various methods to analyze the polarization fluctuation data. We have found that by first constructing the polarization function and then calculating the autocorrelation function, we can obtain the rotational motion of the molecule with very little interference from the lateral diffusion of the macromolecule, as long as the rotational diffusion is significantly faster than the lateral diffusion. Surprisingly, for common fluorophores the autocorrelation of the polarization function is relatively unaffected by the photon statistics. In our instrument, two-photon excitation is used to define a small volume of illumination where a few molecules are present at any instant of time. The measurements of long DNA molecules labeled with the fluorescent probe DAPI show local rotational motions of the polymers in addition to translation motions of the entire polymer. For smaller molecules such as EGFP, the viscosity of the solution must be increased to bring the relaxation due to rotational motion into the measurable range. Overall, our results show that polarized fluorescence correlation spectroscopy can be used to detect fast and slow rotational motion in the time scale from microsecond to second, a range that cannot be easily reached by conventional fluorescence anisotropy decay methods. *Microsc. Res. Tech. 65:205–217, 2004.*

INTRODUCTION

The dynamics of large macromolecules is a field of intense study because of its implications in fundamental phenomena of life. The study of the time scale of rotational diffusion or segmental motions of long polymers or large proteins by standard fluorescence methods such as fluorescence anisotropy is limited by the lifetimes of the fluorescent probe used. Since these probes rarely have lifetimes longer than 10 nanoseconds, one cannot use these methods to measure long rotational times or segmental motions in the microsecond time range. This limitation is particularly important for measurements of large proteins, protein-nucleic acid complexes, and the rotational diffusion of proteins in membranes in which the membrane local viscosity slows down the thermally activated rotational motion. Most studies of rotations of large macromolecules have been performed using phosphorescence probes, which have triplet state lifetimes in the microsecond to second time range. Although these probes are clearly useful, their application is limited by the chemistry necessary to label macromolecules in cells. In addition, due to the long lifetime of these probes, the oxygen concentration needs to be controlled to avoid quenching, which could be inconvenient for studies in cells. There is an alternative method to determine rotational diffusion constants of large macromolecules that is based on fluorescence correlation spectroscopy (FCS), a technique that measures the time-dependent fluctuation in the fluorescence intensity (Aragon and Pecora, 1975; Elson and Madge, 1974; Magde et al., 1972, 1974). In the polarized beam of a laser, the fluorescence intensity will fluctuate because of the angular dependence of the fluorophore's absorption, the orientation of the excitation dipole, and the time-dependent change (relaxation) of this orientation. In this case, fluorescence fluctuations are independent of the excited state lifetime, and it should be possible to measure rotational motions far outside of the fluorophore's fluorescence lifetime. Carried out with polarized light, an FCS experiment will then follow the direction of the absorption (and emission) transition dipole moment through time, one molecule at a time. If there is a

Correspondence to: Enrico Gratton, Laboratory for Fluorescence Dynamics, Department of Physics, University of Illinois at Urbana-Champaign.
E-mail: egratton22@yahoo.com

Received 27 September 2004; accepted in revised form 10 October 2004

Contract grant sponsor: NIH; Contract grant numbers: CMC PHSSUBUVGC 10641 and PHS 5 P41-RRO3155; Contract grant sponsor: Ricerca Ateneo; Contract grant number: 2002-6059004.

DOI 10.1002/jemt.20121

Published online in Wiley InterScience (www.interscience.wiley.com).

polarization of the excitation, then the amount of fluorescence emitted depends on the direction of the absorption transition dipole moment with respect to the polarization direction of the excitation laser beam. Even if the emission is depolarized or if the emission is not observed, using polarizers the fluorescence intensity should fluctuate as the direction of the absorption transition dipole changes. Therefore, an FCS experiment performed using polarized light should carry information about the rotation of the molecule. As a control, we can use unpolarized light or circularly polarized light for excitation. A global analysis of the fluctuation spectra under these two conditions can recover the relaxation due to specifically rotational motion only.

There are other ways to detect the rotational motion of molecule in the FCS experiment, for example using polarized light for excitation and observing the emission using orthogonal polarizers in front of two detectors. In this case, the molecule emission can be detected either by one of the detectors or by the other depending on the orientation of the emission transition dipole moment. The cross-correlation between the signals measured by the two detectors has a characteristic behavior that depends on the rate of rotation of the molecule. In this report, we perform simulations of the different modes of detecting rotations. We also describe experiments using a long DNA polymer with a fluorophore bound in a preferential direction with respect to the axis of the polymer and using EGFP (enhanced green fluorescence protein) molecules in highly viscous media. For the simulations and the measurements, we allow for the translational diffusion of the molecule since the experiments were performed with molecules in solutions rather than restricted on a surface. We later discuss the effect of several fluorophores in the field of excitation both free and when bound to the DNA or to other large macroscopic objects.

FCS has been used to study a wide variety of problems ranging from hydrodynamics to reaction kinetics (Aragon and Pecora, 1976; Magde et al., 1974). Previously, both FCS, and time-resolved fluorescence anisotropy of long lifetime probes have been used to study the rotational diffusion of small molecules in solution (Kask et al., 1987, 1988; Mets 2001). Time-resolved fluorescence anisotropy studies are limited to the lifetime of the probe, often in the nanosecond range. However, there have been only a few experiments in FCS exploiting the polarization of the excitation to study the rotational motions of macromolecules free in solution (Kask et al., 1987, 1988; Mets, 2001). Since FCS is not limited by the lifetime of the probe, then there should be no size limit to the types of molecular aggregates that could be studied by polarized FCS experiments.

FLUORESCENCE CORRELATION SPECTROSCOPY

FCS exploits changes in fluorescence intensity to determine rate processes in a chemical system (Aragon and Pecora, 1975; Magde et al., 1972, 1974). These fluctuations are caused by several factors including dynamic quenching of fluorescence, translational diffusion that brings the molecule in and out of the excitation beam and rotational diffusion. In a typical FCS measurement, the time series of the fluorescence signal from one or more detectors is recorded. The spectrum of the fluctuations is characterized by the autocorrelation function, which is the Fourier transform of the power spectrum of the time series. The autocorrelation function (ACF) is defined by the following mathematical operation

$$G_{ij}(\tau) = \frac{\langle dF_i(t) \cdot dF_j(t+\tau)\rangle}{\langle dF_i(t)\rangle\langle dF_j(t)\rangle} \tag{1}$$

where dF indicates the fluctuation of the fluorescence with respect to the average and the brackets indicate time averages. τ is the delay time between points in the time series. The indices i,j indicate different detectors. For the autocorrelation function, $i = j$. For the cross-correlation function, $i = 1$ and $j = 2$. A characteristic feature of the correlation function is that at short delay times, the correlation of the fluctuation is relatively large since the fluctuation intensity persists for a certain characteristic time. At long delay time, the intensity fluctuation is not statistically correlated to previous fluctuations and the correlation function tends to vanish. In common practice, we calculate the correlation function of the direct time series of the intensity measured by the detector. In the case of polarized emission, we could consider an instantaneous measurement of the polarization and then calculate the spectrum of the fluctuations of the polarization function. The instantaneous fluorescence intensity is relatively small and the mathematical operation of calculating first the polarization and then the fluctuation spectrum at each point in the time series could be subject to errors when the signal is weak. However, our simulations show that the effect of the statistics is less important than that expected just on the basis of the above consideration. In the next section, we will examine the advantages and limitations of measuring the spectrum of the fluctuations of the polarization rather than the individual (polarized vs. unpolarized) fluctuation spectra.

FLUCTUATIONS DUE TO TRANSLATIONAL AND ROTATIONAL DIFFUSION

The correlation function due to translational diffusion through a 3D Gaussian beam profile formed by two-photon excitation is given in the following expression (Thompson, 1991).

$$G_D(\tau) = \frac{\gamma}{N}\left(1 + \frac{8D\tau}{w_o^2}\right)^{-1}\left(1 + \frac{8D\tau}{w_z^2}\right)^{-1/2} \tag{2}$$

In this equation, γ is a geometrical factor that accounts for the shape of the excitation profile, N is the average number of molecules in the volume of excitation, D is the diffusion coefficient in $\mu m^2/s$, and w_o and w_z are the beam waists in the radial and axial direction in μm, respectively. In most of our experimental conditions, we found that w_z was about 5 times w_o and that w_o, which depends on the wavelength and on the numerical aperture of the objective, is typically around 0.35 μm. The characteristic time for a particle to transverse the excitation volume is given by the following expression (for 2-photon excitation)

$$\tau_c = \frac{w_o^2}{8D} \tag{3}$$

For EGFP, the diffusion coefficient in water at room temperature is about 95 $\mu m^2/s$ and if the beam waist is 0.35 μm, then the characteristic transit time is about 160 μs.

If the rotational and the translation motion are independent, then the total correlation function factorizes in two separate terms. The expression for the rotational diffusion part of the correlation function is complex and it depends on several factors, including the angle between the excitation and emission transition dipole moments, the polarization of the excitation, and the observation using emission polarizers. In the simplest case, where the excitation and emission transition dipole moments are parallel (this also implies that the molecule does not rotate during the excited state lifetime), the sample is excited with polarized light and the emission is observed without polarizers, the complex expression for the rotational correlation function takes the simple form (Ehrenberg and Rigler, 1974; Mets, 2001)

$$G_R(\tau) = a_0 + b_0 \exp(-\tau/\tau_R) \tag{4}$$

The total correlation function is then given by

$$G(\tau) = G_R(\tau) \cdot G_D(\tau) \tag{5}$$

Expression (5) indicates that the rotation can only be observed at delay times where the translation term is greater than zero, since the rotational term (4) is always greater than zero. In other words, the rotational correlation time must be similar or faster than the mean diffusion time through the volume of excitation. In principle, if the rotational correlation time is slower than the characteristic transit time, the laser beam profile could be expanded to bring the two characteristic times into the same range, since diffusion time depends on the size of the beam waist while the rotational times is independent on the beam waist.

We note that the above equations are only valid for small particles (compared to the beam profile), for isotropic rotation, and for particular conditions of excitation and emission polarizer directions. The expressions for isotropic and anisotropic rotational diffusion as well as the expressions for non-co-linear excitation and emission transition dipoles and for different directions of excitation and emission polarizers have also been reported (Ehrenberg and Rigler, 1974). For the FCS experiment, the geometry for excitation and observation is the same due to the epi-illumination optics. The only variables are the polarization of the excitation and whether or not the emission is split into components that are parallel and perpendicular to the polarization of the excitation light. However, the form of the total correlation function given by the product of the lateral and rotational diffusion terms does not depend on the particular rotational model used and on the observation conditions.

SINGLE PARTICLE POLARIZED FCS SIMULATIONS

Simulations were performed using the SimFCS program developed at the Laboratory for Fluorescence Dynamics at the University of Illinois at Urbana-Champaign. This program can be downloaded from our web site (www.lfd.uiuc.edu). The core of the simulation program is based on particles performing a random walk on a grid. The grid has a size of 50 nm per point and it extends for 128 points in a cubic lattice for the simulations performed in this report. The size of the grid and the total volume of the simulation can be changed by the user. At the center of the grid, there is a volume of illumination described by a 3D Gaussian profile with a radial waist w_o and an axial waist 5 w_o. The particles perform lateral diffusion with a characteristic diffusion constant that varies depending on the simulation between approximately 100 to 0.01 $\mu m^2/s$ and a rotational motion with a characteristic rotational correlation time in the range 1 μs to 4 s depending on the simulation. The rotational motion is simulated by the random walk of a dipole on the surface of a sphere. The sphere is covered with a grid of equal angular extent. The size of the angular grid can be changed by the user. For the simulations of this work, the angular grid was 18 degrees.

The emission is observed by two detectors that can be either unpolarized or with orthogonal direction polarizers. The excitation is either unpolarized or linearly polarized in the vertical direction. It is assumed that the absorption is due to a linear dipole and the emission is co-linear with the absorption. The grid is filled with 1,000 independent molecules unless otherwise stated. The sampling frequency for the fluorescence detection was set anywhere between 10 MHz to 10 kHz, depending on the simulation.

Using simulations of the rotational diffusion, we show the effect of rotational relaxation on the correlation function obtained using different conditions for excitation and emission polarizer directions.

Figure 1 shows the intensity profile (bottom curve) under conditions of unpolarized excitation and unpolarized emission. For this simulation, the particle is diffusing with a diffusion coefficient of 1 $\mu m^2/s$ and simultaneously rotating with a characteristic rotational correlation time of approximately 250 μs. The simulation was performed with a sampling frequency of 40 kHz. Actually, there are two lines superimposed corresponding to the intensity detected by the two channels in Figure 1. The intensity in Figure 1 is averaged over 1,000 time bins corresponding to 25 ms, although the data are simulated each 25 μs. The upper curve in Figure 1 is the plot of the polarization defined as

$$P = \frac{I_V - I_H}{I_V + I_H} \tag{6}$$

The indexes V and H indicate vertical and horizontal polarization detection with respect to vertical polarized excitation if used, respectively. The emission polarization should be zero since the excitation light is unpolarized for this simulation, and the emission polarizers have been removed. However, due to statistical effect when the intensity is very small, the apparent polarization differs from zero. However, the fluctuation of the polarization is not correlated since it is due to noise. The large fluorescence fluctuations in Figure 1 are due to the passage of bright molecules in the volume of excitation.

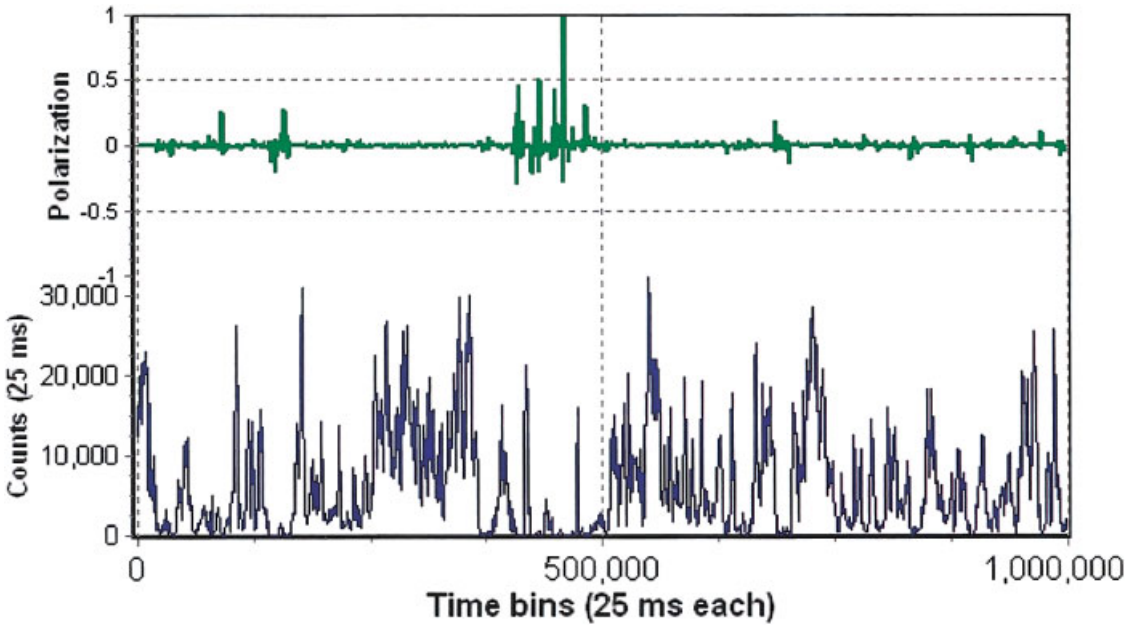

Fig. 1. Fluorescence intensity (bottom curve) and polarization (top curve). The simulation is performed with a sampling time of 25 μs. In the graph, 1,000 points are added for each point. In the simulation, the excitation light is unpolarized and the emission polarizers have been removed. [Color figure can be viewed in the online issue, which is available at www.interscience.wiley.com.]

The autocorrelation functions for both channels and the cross-correlation between the two channels are identical, and they correspond to the ACF using the unpolarized excitation curve of Figure 2. Next, we added the excitation polarizer.

In Figure 2, we report the ACF using vertically polarized excitation and the ACF of the polarization function. Because there are no polarizers in emission, the individual ACF for each channel and their cross-correlation functions are identical. The autocorrelation function of the polarization when no polarizers are used has no specific features since the noise in this curve is uncorrelated. The apparent value of the ACF of the polarization is large (curves are plotted normalized in Fig. 2) due to the average value of the polarization, which is nearly zero. Since the rotational correlation time for this simulation is fast compared to the diffusion time through the excitation beam profile, the relaxation process due to the fluctuations of the transition dipole direction appears very distinct in the ACF function at short times (Fig. 2). In other words, during the transit of the molecule in the excitation volume, the rotational relaxation is complete. The curves with and without polarizers differ at short times only, because the ACF obtained using polarized excitation has an additional fast relaxation due to the rotational motion. The amplitude of this extra relaxation depends on the polarization of the molecule as discussed by Mets (2001). For a linear dipole, the ratio between G(0) with and without polarized excitation should be less than a factor of 2. For planar absorbers or lower symmetries, this ratio could be lower and even less than 1.

Next, we added the emission polarizers (in the parallel and perpendicular orthogonal directions) in the two detection channels, leaving the excitation polarizer parallel. The results of the simulations are shown in Figure 3.

The autocorrelation of both emission channels is identical but their cross-correlation has now a different trend with a rise at short correlation times. This phenomenon is generally termed anti-correlation or anti-bunching. It is due to the fact that when a molecule emits in the parallel direction, it cannot emit in the perpendicular direction and vice versa. We also report the curve for the ACF of the polarization function. Note that in this curve the relaxation due to lateral diffusion, which occurs around 40 ms, is absent. Instead, the lateral diffusion process is visible as the relaxation at longer times in each of the ACF intensity curves in Figure 3. The rotational diffusion process is independent of the lateral diffusion. However, it could be difficult separating the two terms if the two times (for rotation and for diffusion) are similar.

In the following simulation, we examine the case in which the rotational motion occurs on the same time scale of the transit time of the molecule through the excitation volume. In the simulation, we slowed down the rotational correlation time by a factor of one thousand, maintaining the same beam transit time (Fig. 4).

This simulation shows that when the rotational correlation time (400 ms) is much larger than the transit time (40 ms), the rotational relaxation process is difficult to discern. The cross-correlation function, as well as the ACF of the polarization, shows a definite shift toward longer times although their apparent relaxation is far from the expected 400 ms used for the simulation.

Since the ACF of the polarization function seems to be very effective in canceling the effect of the transla-

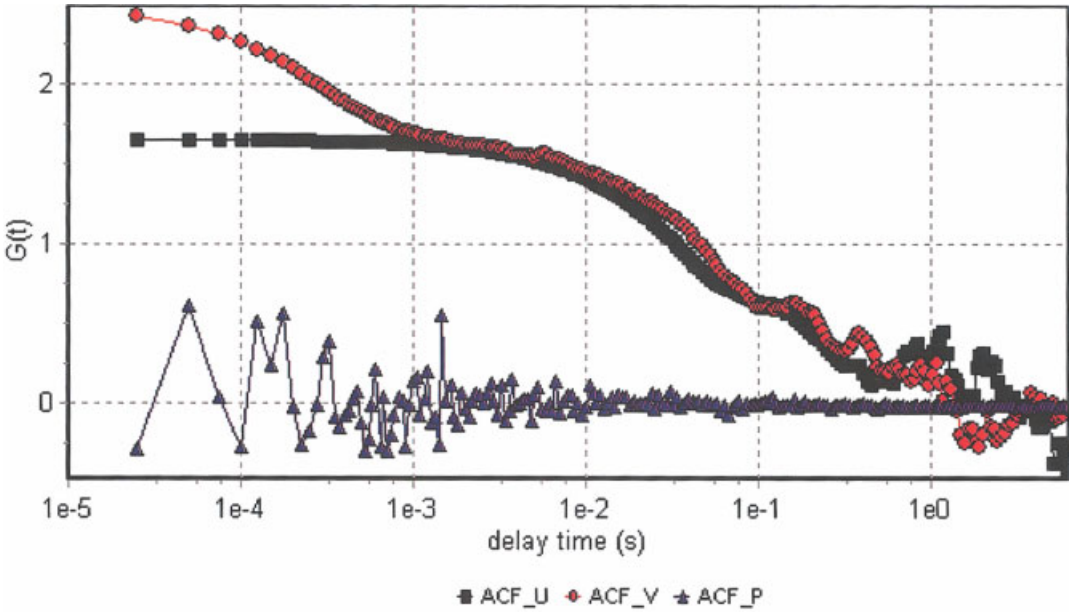

Fig. 2. Squares: ACF using unpolarized excitation; circles: ACF using vertically polarized excitation; triangles: ACF of the polarization function. [Color figure can be viewed in the online issue, which is available at www.interscience.wiley.com.]

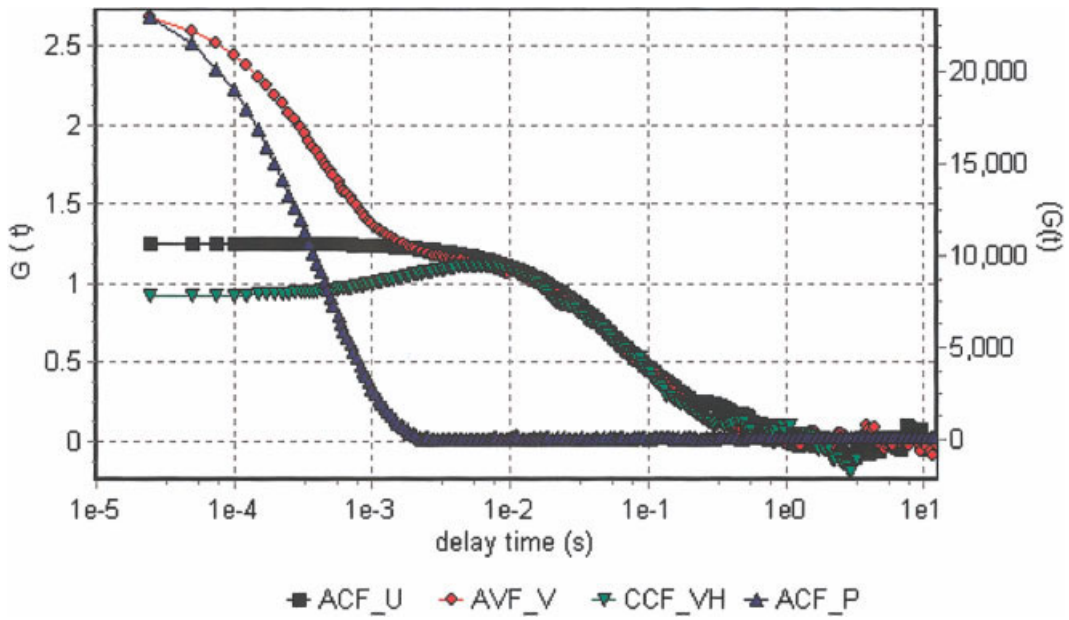

Fig. 3. Squares: ACF using unpolarized excitation; circles: ACF using vertically polarized emission; down triangles: cross-correlation between the two orthogonal emission channels; up triangles: ACF of the polarization function. [Color figure can be viewed in the online issue, which is available at www.interscience.wiley.com.]

tional diffusion, we performed a systematic study using simulations in which the rotational correlation time is changed from 0.4 ms to 4s in factors of 10 while the residence time in the excitation volume was kept constant at 40 ms (Fig. 5).

The calculation of the ACF of the polarization function gives the correct value of the rotational correlation time until the residence time of the particle in the illumination volume increases to approximately 1/10 of the rotational correlation time. For very slow rotational correlation times (in the presence of fast lateral diffusion), the rotational relaxation cannot be seen any more as a separate relaxation and the resulting ACF curves no longer reflect the rotational motion of the

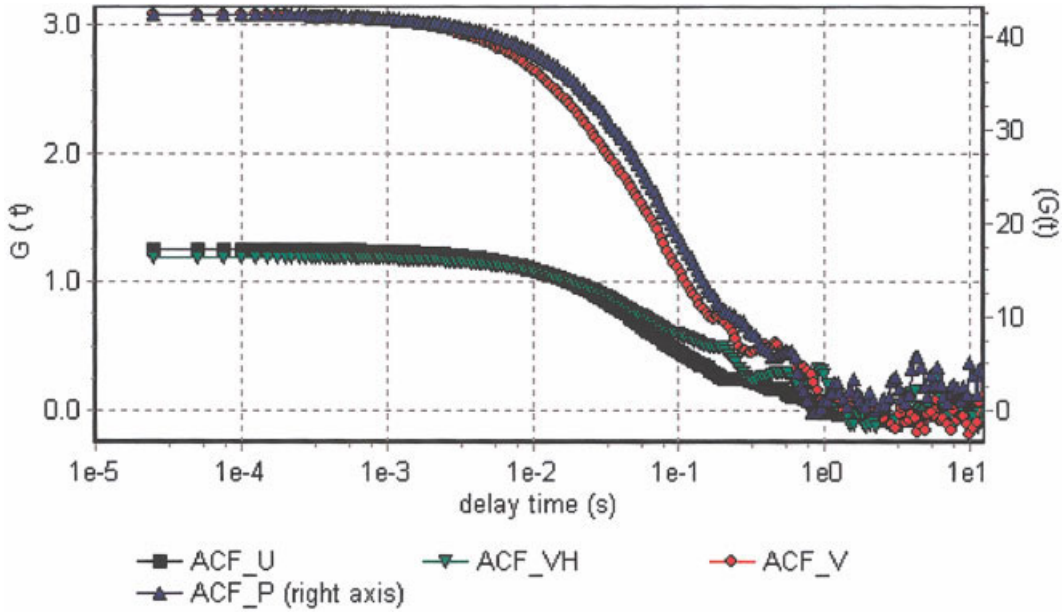

Fig. 4. Squares: ACF using unpolarized excitation; circles: ACF using vertically polarized excitation; down triangles: cross-correlation between the two orthogonal emission channels; up triangles: ACF of the polarization function. [Color figure can be viewed in the online issue, which is available at www.interscience.wiley.com.]

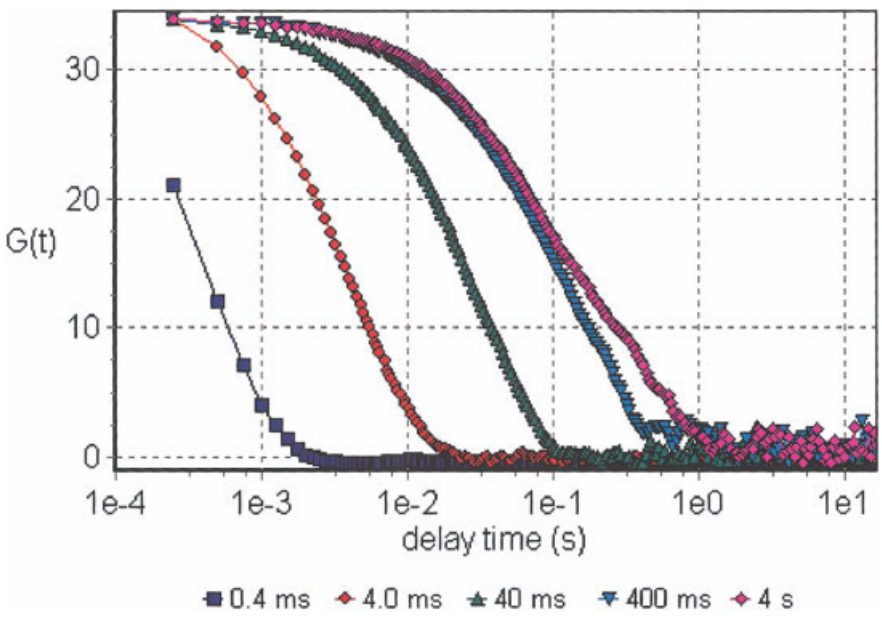

Fig. 5. Normalized ACF of the polarization after binning the time data series by 10. The approximate value of the rotational correlation time was changed by a factor of 10 for each successive simulation according to the legend. The beam transit time for the particle was constant with a residence time of approximately 40 ms. [Color figure can be viewed in the online issue, which is available at www.interscience.wiley.com.]

particle, only the beam transit time. As we discussed previously, experimentally it should suffice to enlarge the illumination profile to allow some of the rotational relaxation to occur during the transit time through the illumination volume.

We have demonstrated that we can easily detect the rotational relaxation process using the autocorrelation of the polarization if it occurs during the beam transit time. However, the particles used for the simulations were very bright. In the following, we perform simulations for particles with different brightness to determine the effect of the counts statistics on the autocorrelation of the polarization function (Fig. 6A).

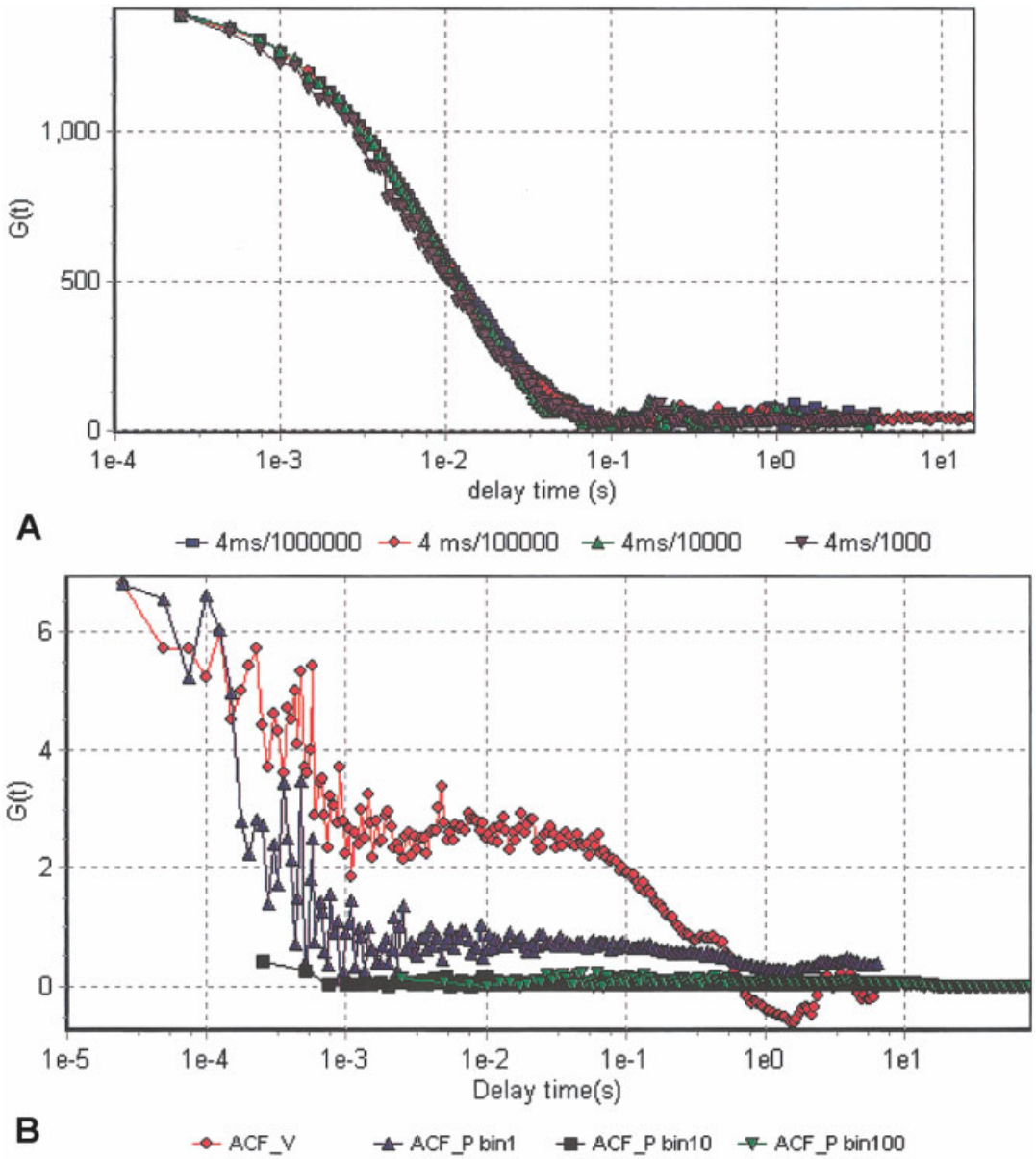

Fig. 6. **A:** Normalized ACF of the polarization for different count rates in the range of common measurements from 1,000 to 10,000,000 c/s according to the legend. For this simulation, the rotational correlation time was 4 ms and the transit time was 40 ms. **B:** Effect of data binning at very low count rate and very fast rotational diffusion. Circles: ACF of the vertical polarization; up triangles: ACF of polarization; squares: ACF of polarization binned by 10; down triangles: ACF of polarization binned by 100. [Color figure can be viewed in the online issue, which is available at www.interscience.wiley.com.]

We changed the brightness from 1,000,000 count/s/molecule (corresponding to a DNA molecule with many fluorophores attached) to 1,000 count/s/molecule (less than the brightness of an EGFP molecule in our instrument, which is about 3,000 count/s/molecule), covering the useful range of most practical measurements. It appears that the count statistics does not affect the shape of the curve due to rotational relaxation, although the amplitude of the ACF of the polarization function changed somewhat between simulations. We note that the amplitude of the AFC depends on the average value of the polarization, which was dependent upon the particle brightness due to count statistics. Surprisingly, the normalized ACF of the polarization seems to be a robust function, useful to determine the rotational correlation time from the fluctuation of the polarization, independently of the count statistics in the range examined. Of course, the rotational relaxation must be able to occur during the transit time in the excitation profile. For this simulation, the rotational correlation time was fixed to approximately 4 ms. We then decreased the rotational correlation time to approximately 100 μs, increased the beam transit time to 400 ms, and set the particle brightness to

1,000 counts/s/molecule. We also decreased the integration time to have an overall poor statistics. Although the ACF of the polarization picks up the rotational relaxation very well, as shown in Figure 6B, we note that under these conditions of poor statistics there is a contamination due to the translational diffusion that can be seen as a relaxation at a longer delay time in the autocorrelation of the polarization curve. However, if we increase the statistics by a factor of 10 or 100 by binning time points by 10 or 100, this effect disappears. It is important that we distinguish between an effect due to poor statistics from a real effect in which the rotational diffusion is very slow and superimposed on the diffusion term. To recognize this effect, we should trying binning the data and see if the "better" statistics of the binned data makes the contamination to disappear. This contamination only occurs if the rotational correlation time is very short and the statistics of counts is poor. Data binning is done after data collection, i.e., this test can be performed on data already acquired if the statistics was poor.

MULTIPLE PARTICLES OR MULTIPLE FLUOROPHORES ON THE SAME MACROMOLECULE

Until now, we have considered a single fluorophore freely rotating in 3D space. There are at least two other systems that we will discuss. In both systems, we have a number of identical fluorophores bound to some macromolecular structure. In the first case, we have a fluorophore (DAPI) bound to a linear polymer (DNA). If there are many fluorophores simultaneously on the volume of illumination rigidly attached to a certain structure, as this structure rotates in the polarized excitation beam, there is no change in the fluorescence emitted if each fluorophore is randomly oriented with respect to the others. As we will see later in this report, DAPI binds in the minor groove of the double helical DNA. This kind of binding gives a local preferential organization to the average orientation of DAPI molecules. As a consequence, there is a local correlation of orientations of DAPI molecules. The local orientation has a spatial correlation that depends on the persistence length of the DNA (Barcellona and Gratton, 1996a,b). For the polydeoxynucleotide we used and under the specific experimental conditions, the persistence length is approximately 70 nm, smaller that the waist of the laser beam at the focal point but sufficient to give a local orientation. In our experimental conditions, the concentration of the dye is such that the DNA molecule is almost completely decorated with DAPI molecules. Of course, there is also free DAPI in solution, but the fluorescence of free DAPI is an order of magnitude less than the fluorescence of bound DAPI and the rotational correlation time of free DAPI is in the picosecond time scale while the changes in orientation of the large DNA molecule along the polymer axis are in the microsecond to millisecond time scale. Another system of great interest is constituted by membrane rafts in which a relatively large patch in the membrane could behave as a rigid structure from the point of view of the lateral diffusion. We don't really know yet if proteins in a raft can rotate in the plane of the membrane or if the entire raft can rotate. We know instead that the permanence time of a raft in the laser beam is on the order of 10 to 100 s (Inoue et al., 2004). If we only have one or a few fluorescence molecules in a raft, we should be able to detect the rotational rate of the molecule in the raft. Instead, if the raft has many fluorescent proteins presumably not aligned in the same direction, then the fluorescence fluctuations due to rotational motions should wash out.

Therefore, the condition to observe the rotational behavior of a relatively large structure is either having many fluorophores that are preferentially aligned by the underlying structure or having only a few fluorophores in the volume of excitation (ideally only one) such that the behavior of the single fluorophore can reveal the rotational motion of the structure to which it is attached.

MATERIALS AND METHODS

Polyd(AT) of average 10,000 bp long was acquired from Sigma (St. Louis, MO). 4′-6-Diamidine-2-phenylindole dihydrochloride (DAPI) was obtained from Molecular Probes (Eugene, OR). EGFP gene was obtained from BD Biosciences Clontech (Palo Alto, CA), and cloned with six histidines on the C-terminal end. It was expressed in BL21DE3 *Escherichia coli* strain and purified to homogeneity with 6xHis-tag/Ni-NTA resin, Qiagen Sciences Inc. (Germantown, MD) according to the manufacturer's protocol. For these experiments, we diluted the EGFP to a concentration of 10 nM. Plasmid DNA of the PKC delta gene, a kind gift from Prof. Wonhwa Cho, at the University of Illinois, Chicago, was cleaved with the restriction enzyme PvuII to provided DNA fragments of 400 and 200 bp. The various fragments were purified using a Qiagen Sciences Inc. miniprep plasmid purification kit according to the manufacturer's protocol. Only the 200-bp fragment was used in this work.

All reagents were of the highest purity available and doubly distilled water, Millipore filtered, was used throughout. The concentration of the solutions was determined by using the following molar extinction coefficients: 6,600 M^{-1} cm^{-1} at 262 nm for the plasmid DNA and for the polyd(AT), 23,000 M^{-1} cm^{-1} at 342 nm for the DAPI. The absorption ratio A_{260}/A_{280} was 1.8, providing an estimation of polymers purity.

The experimental solution for the polyd(AT) sample contained DAPI at 2 μM and a phosphate concentration (as DNA base) of 1 μM in aqueous buffered solution of 50 mM Tris, 1 mM EDTA, 100 mM NaCl at pH 8. Under this condition, the DNA is almost fully decorated with DAPI. The solution was divided in two parts and one was placed in a 90°C water bath for 5 minutes. After heating, the sample was put into an ice bath at 0°C for 5 minutes. This should have induced the formation of hairpins in the DNA. DAPI has high fluorescence intensity when bound to A-T segments of DNA, and it has very low fluorescence intensity when free in solution.

It has been previously shown that DAPI binds tightly to AT-rich regions (Manzini et al., 1983; Wilson et al., 1990) and it maintains a specific angle with respect to the helical axis (Barcellona and Gratton, 1996a,b) (Fig. 7).

For the purpose of the rotational studies of this report, DNA can be modeled in three basic ways: as a locally rigid rod, a weakly bending rod at a larger

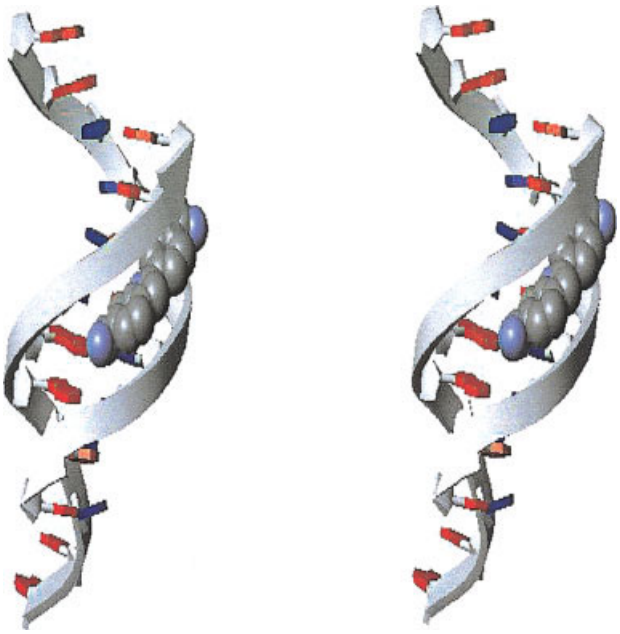

Fig. 7. Schematic representation of the DAPI bound to polyd(AT). [Color figure can be viewed in the online issue, which is available at www.interscience.wiley.com.]

dimension, or a flexible polymer for very long structures. Because DNA probably acts like combinations of all of these models, a closed form solution of the autocorrelation function or of the rotational diffusion time would not be appropriate. Models for the bending and torsional motions and the expressions for the correlation functions were previously derived (Barcellona and Gratton, 1996a,b; Ermak and McCammon, 1978; Hongmei et al., 1997; Schurr and Fujimoto, 1988; Schurr et al., 1992). However, the purpose of the present study is to establish the methodology for polarized FCS rather than to study the flexibility of the DNA molecule so that specific fitting models were not employed.

For the 200-bp plasmid fragment, the labeling ratio was P/D = 20. The plasmid fragment has only 2 sites were DAPI can bind. Under our experimental condition, we should have at most one DAPI dye per DNA fragment.

FCS Apparatus

The two-photon excitation FCS fluorescence microscope used in these experiments was assembled at the Laboratory for Fluorescence Dynamics. The experimental setup, although using a different microscope body, was previously described (Berland et al., 1995). Briefly, a mode-locked titanium-sapphire laser with 80-MHz, 100-fs pulse width (Tsunami; Spectra-Physics, Palo Alto, CA) was used as the excitation light source. The laser was spatially filtered and brought to the back port of a Nikon Eclipse, TE300 microscope (Nikon, Japan). The primary dichroic from Chroma Technologies (Battleboro, VT) 700DCSPXR reflects the laser up to the sample and passes the epi-collected fluorescence. The dichroic cutoff is 700 nm. This light is then focused on the input pinhole of the ALBA FCS correlation module by ISS Inc (Champaign, IL). This module has a polarizing beam splitter that splits the light into orthogonal components detected by 2 identical GaAs cooled H7422P/40 Hamamatsu (Japan) photodetectors. A BG39 optical filter from Chroma Technology was placed before the ALBA unit for efficient suppression of IR excitation light. A Zeiss (Thornwood, NY) 40X Fluar (1.3 N.A.) oil immersion objective lens was used for all measurements. The excitation was either linearly polarized (the natural mode of the laser) or circularly polarized using a quarter wave plate. Excitation wavelength ranged from 790 nm for the DAPI samples to 930 nm for the EGFP samples. Data were collected by the FCS-PCI dual channel card (ISS Champaign, IL) in the photon mode and further analyzed using the SimFCS software (LFD, Urbana, IL). The excitation volume depends on the wavelength and of the objective. Typically, we obtained volumes in the 0.1–0.2 fL range.

Fluorescence Measurements on Polyd(AT) Samples

Four FCS experiments were performed on each sample. Two measurements were performed with no polarizer in the emission side and either unpolarized light or vertically polarized light was used for excitation. Two additional experiments were performed using the beam split polarizer in the emission side and alternating the excitation between unpolarized and vertically polarized light. FCS data collection for the polyd(AT) sample was performed at 40 kHz, for a total collection time of about 1,000 s.

RESULTS

Figure 8 shows the raw data for a small period of data acquisition for the polyd(AT) sample 1. For this data set, the two detectors have polarizers in front and excitation is done with vertically polarized light. Comparison with the simulated data of Figure 1 shows that there is a similar structure in which large intensity fluctuations are visible. The total intensity is different from that of the simulation because the brightness of the particles is much less in the experiment than in the simulation. We also note that the polarization is negative in the experimental condition. This is due to different efficiencies of the two detection arms.

The calibration of the polarization efficiency was performed using a solution of fluorescein, which has very low polarization at room temperature in water. For fluorescein, the ACF of the polarization was flat. The raw polarization of fluorescein as measured in our instrument was about −0.125. From this value, a calibration g-factor for the polarization function was calculated to be 0.778. For each experimental condition, the g-factor was calculated using fluorescein as a standard and the correction factor was successively applied to all collected data for that day. In practice, in this report we only use qualitative considerations based on the rotational correlation time rather than on the amplitudes of the polarization function. Therefore, the calibration of the polarization function is used as a comparison (with fluorescein) to determine if the emission is polarized or not.

The data of Figure 8 were used to calculate the various correlation functions described in the first part of this article. In Figure 9, we report the ACF for polyd(AT) sample 1 for vertically polarized excitation

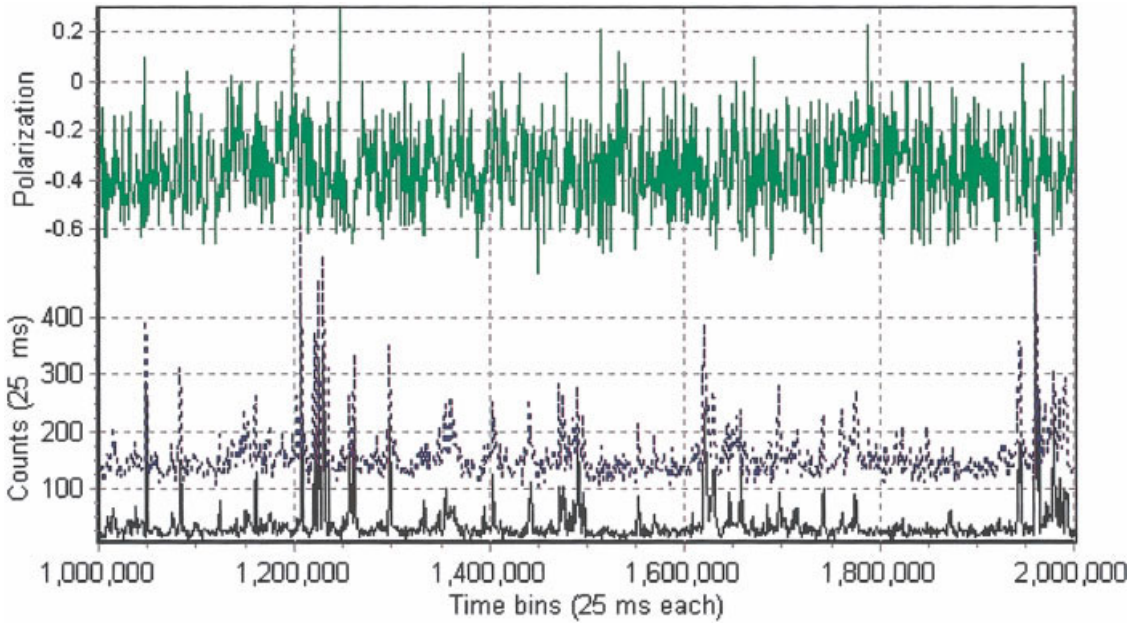

Fig. 8. Time series of a small portion of the data collected for polyd(AT) sample 1. **Bottom:** The dotted and solid lines are for the emission vertical and horizontal polarization direction, respectively. The dotted line has been displaced vertically to make it distinguishable. **Top:** The value of the raw polarization calculated for each time bin. The average polarization is negative due to calibration issues. [Color figure can be viewed in the online issue, which is available at www.interscience.wiley.com.]

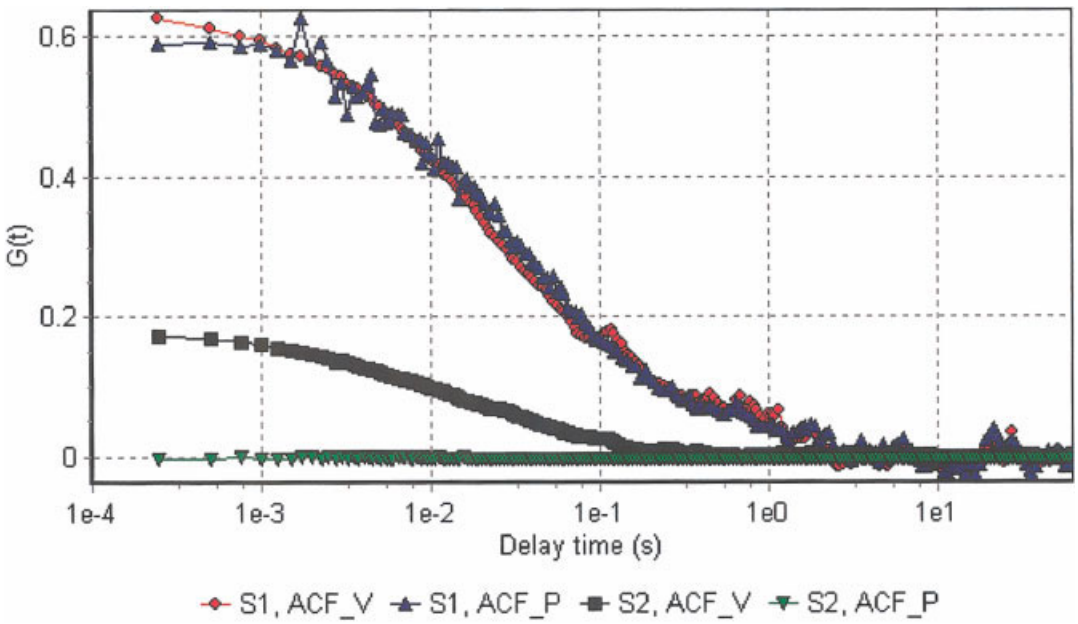

Fig. 9. Comparison between polyd(AT) sample 1 and sample 2. ACF of sample 1 (circles) and ACF of sample 2 (squares) for vertically polarized emission (excitation is vertically polarized). Up and down triangles: ACF of the polarization of sample 1 and 2, respectively. Original data series has been binned by 10 to increase the statistics. [Color figure can be viewed in the online issue, which is available at www.interscience.wiley.com.]

(no emission polarizer) and the ACF of the polarization function when the emission polarizers were inserted.

The average transit time in the volume of illumination is about 25 ms. The ACF of the polarization lies almost on top of the ACF for polarized excitation, indicating that for this sample there is very little relaxation due to rotation of the macromolecule during the beam transit time.

Comparison between sample 1 and sample 2 shows that the translation diffusion of the two samples differs

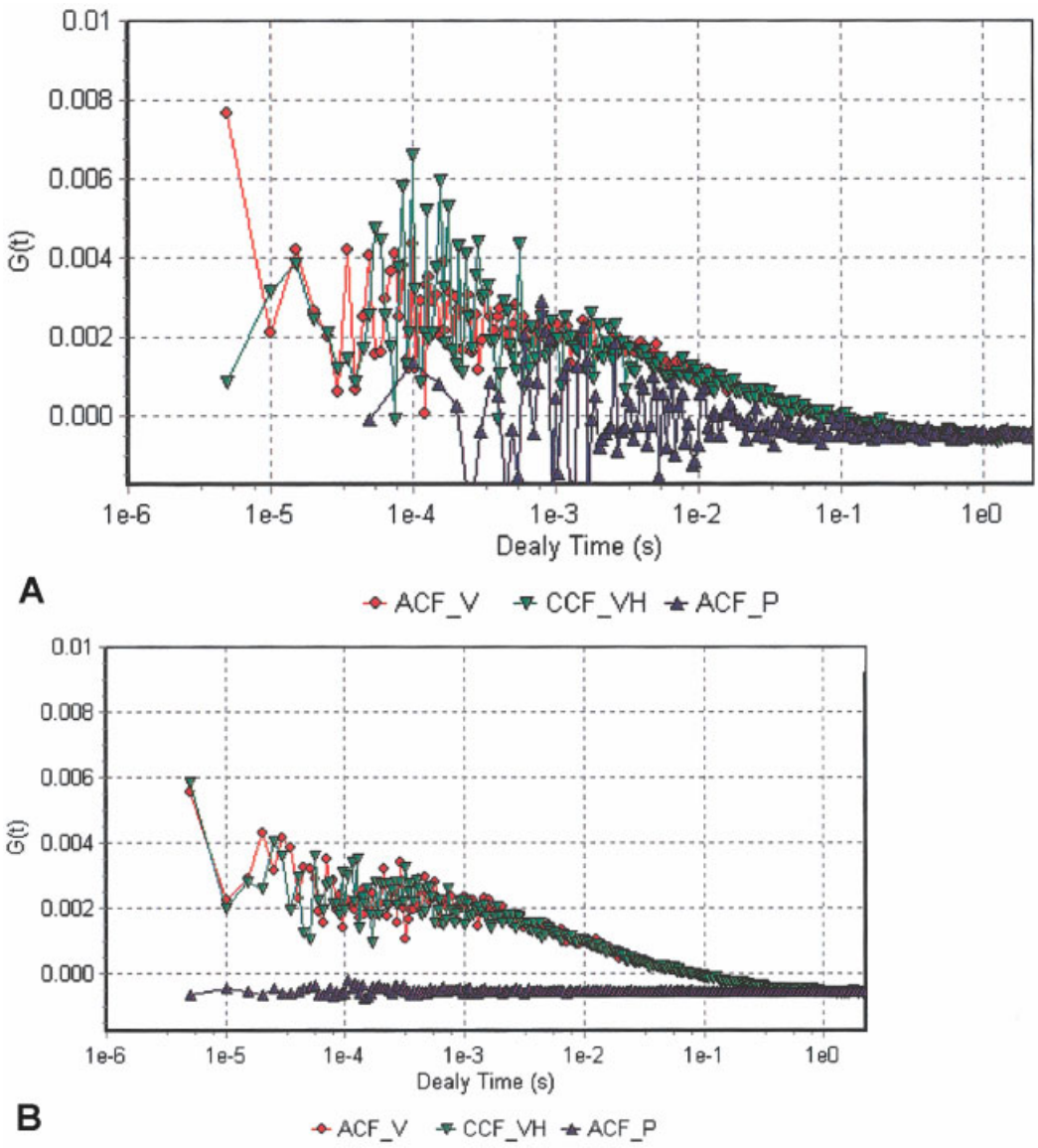

Fig. 10. **A:**. EGFP in glycerol using vertical polarizer in excitation. Circles: ACF for the vertical polarized channel; down triangles: cross-correlation between vertical and horizontal polarized emission; up triangles: ACF of the polarization. Polarization data have been binned by ten due to increase the statistics. **B:** EGFP in glycerol using circular polarizer in the excitation. Circles: ACF for the vertical polarized channel; down triangles: cross-correlation between vertical and horizontal polarized emission; up triangles: ACF of the polarization. [Color figure can be viewed in the online issue, which is available at www.interscience.wiley.com.]

by more than a factor of 2, sample 2 moving faster than sample 1 (Fig. 9). However, for sample 2 the ACF of the polarization is flat, indicating that for this sample the rotational relaxation of the polymer was completed during the transit across the beam profile. Another possibility is that there are too many fluorophores in the polymer and that they are randomly oriented. The steady state polarization of sample 2 is very close to the polarization of the fluorescein control, which is close to zero, while sample 1 has an emission polarization different from zero. The total fluorescence intensity is similar indicating that the number of fluorophores is about the same for both samples. Therefore, we believe that the heat treatment has strongly reduced the size of the aggregates and that for sample 2 the depolarization of the emission is completed during the time we sample the next intensity point. The absolute value of the G(0) is also different between the two samples, indicating that there are more particles in sample 2.

EGFP Measurements in Viscous Solution

Two series of measurements were performed for the EGFP in glycerol. In one series, the excitation light was vertically polarized and for other series the light was circularly polarized. The results are shown in Figure 10A,B, respectively.

The relaxation due to the translational motion is clearly visible with a characteristic transit time of ap-

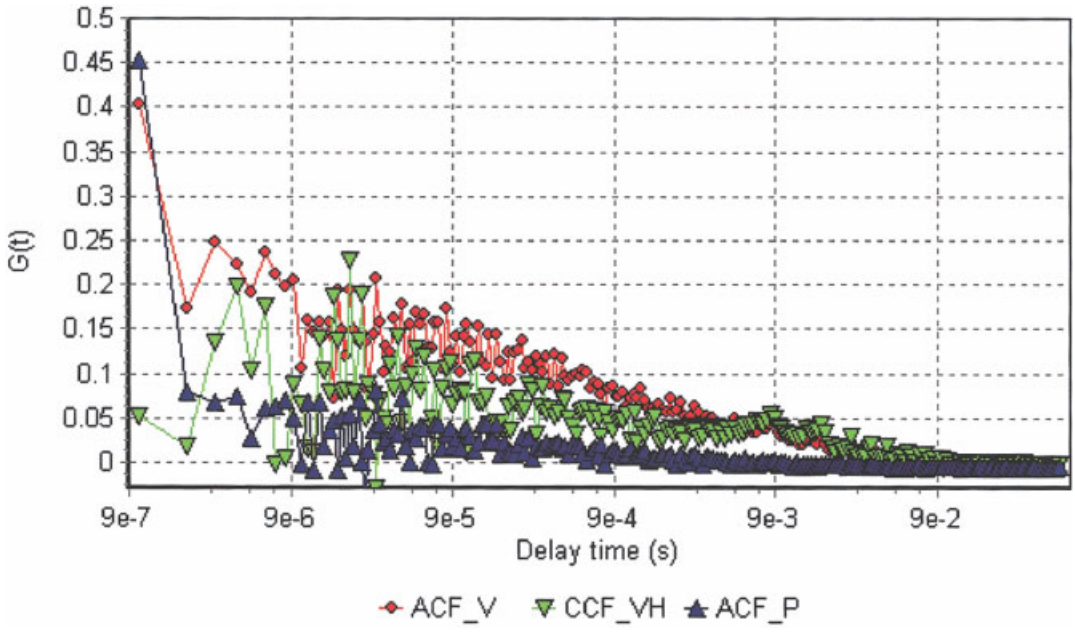

Fig. 11. ACF for the DNA fragment of approximately 200 bp. Circles: ACF for the vertical polarized channel; down triangles: cross-correlation between vertical and horizontal polarized emission; up triangles: ACF of the polarization. [Color figure can be viewed in the online issue, which is available at www.interscience.wiley.com.]

proximately 10 ms. This value indicates that the viscosity is about 70 times that of water. The ACF of the polarization function is flat, indicating that the rotation is completed at times shorter that the minimum sampling time of our data collection. These measurements were performed using a sampling frequency of 200 kHz. Assuming that the viscosity is about 70 cp, the expected rotational correlation time for EGFP based on the molecular weight and the volume of hydration is about 0.7 μs, which is indeed out of the window of our measurement.

Plasmid Measurements

The results of the series of measurements on the 200-bp plasmid DNA with and without excitation polarization are shown in Figure 11. In this case, also the ACF of the polarization increases at shorter times indicating that the rotational diffusion is not entirely complete at the shorter times we have measured. For this set of data, we were able to increase the sampling frequency to 1 MHz

DISCUSSION

In this report, we discuss the measurement of rotational diffusion of macromolecules using polarized FCS. There is more than one way to perform the polarized FCS measurements, depending on the use of polarizers in the excitation and in the emission side. A robust way to detect the rotational diffusion is by using vertically polarized excitation and splitting the emission in two channels each sensitive to an orthogonal direction of polarization. Unless macromolecules are immobilized on a surface, translational diffusion determines the duration of the observation for one molecule. If the rotational relaxation occurs during that time, the relaxation can be observed. Of course, the rotational relaxation could be so fast that the resolution of the rotational diffusion is not achievable using common instruments. However, most of the FCS instruments can acquire data in two channels at frequencies on the order of 1 MHz or faster. This sampling frequency determines the faster rotational correlation time that can be measured and sets a limit for the lower mass of a macromolecule of spherical shape. If the viscosity is that of water, the minimum mass for a spherical shape that can cause a measurable relaxation due to rotation is about 300 kD.

However, in the cell interior the viscosity is about 3–5 times larger than that of water, bringing down the minimum size of a molecule that can be measured to about 60–100 kD. If the macromolecule is elongated, then the rotational correlation time along the long axis is longer. For example, for DNA molecules, the minimum length that can be measured corresponds to 20–50 bp. If the macromolecule is on a membrane, the local viscosity will always bring the rotational motion into the region in which the FCS measurement can be done.

A technical consideration that can limit the range of rotational relaxations that can be distinguished is due to the detector after-pulse. This effect is visible in all our measurements. Using the cross-correlation of the two detectors, after-pulsing can be minimized. This could be a reason to prefer the cross-correlation method for the determination of very fast rotations instead of the autocorrelation of the polarization function.

To extract the contribution of the rotational diffusion from the translational motion, we found that if we first

calculate the polarization function and then calculate the autocorrelation function of the polarization, we can obtain the rotational relaxation contribution almost free from the translational contribution if the rotation relaxation occurs during the molecule transit time in the excitation profile. Remarkably, the ACF of the polarization is very little affected by the photon statistics, at least for the brightness of commonly used fluorophores. A simple check can be performed once data have been acquired to test the influence of photon statistics. If we bin the data by a factor, for example 10, the statistics increases in a given bin. When we now calculate the polarization, the increased statistics will tend to the correct value.

Our experimental results show that polyd(AT) labeled with DAPI before heat treatment rotates very slowly. Heat treatment resulted in sample depolarization which can be caused by an increase in rotational motion. Alternatively, the depolarization can be due to statistical effects from large curvature of the DNA or random orientation of bound DAPI molecules. For a molecule the size of the EGFP, we need to increase the viscosity of the solution to bring the fast rotational relaxation into our window of observation. Due to the maximum viscosity we were able to obtain using glycerol, we were unable to distinctly recognize the rotational relaxation for this molecule. For the experiments with relatively short pieces of DNA (about 200 bp) we were able to increase the sampling frequency to about 1 MHz and we were able to distinguish the effect of a very fast (in the 10-microsecond range) relaxation due to depolarization.

The simulation program we wrote accurately predicts the behavior of rotational relaxation for single fluorophores attached to large macromolecules and it can be used to determine the experimental conditions under which the rotational relaxation can be observed.

In this report, our focus was the detection of a relaxation in the autocorrelation curve due to depolarization motion. Intentionally, we have not attempted to fit the data since we wanted to show that the rotational motion can be directly deduced from the shape of the autocorrelation function. Of course, a quantitative determination of rotational relaxation requires curve fitting according to a model for the rotation. Except for the simplest model of a spherical rotator with coincident axis for absorption and emission, the form of the autocorrelation function for the rotational motion is complex. In general, two or more exponential terms are needed to fit the ACF curve.

In conclusion, polarized FCS provides a powerful method to measure rotational motions of macromolecules in a time range in which the traditional fluorescence methods based on the decay of the emission anisotropy cannot be used due to the limited duration of the excited state lifetime. Since polarized FCS only depends on the orientation of the excitation transition dipole moment, common fluorophores can be employed. However, to exploit the polarization function, the emission must be at least partially polarized. For molecule like EGFP, this is not a problem since the fluorescence lifetime of EGFP is generally much shorter than the rotational correlation time.

If a macromolecule (or large molecular aggregate) has several fluorophores, polarized FCS can only be done if the fluorophores have preferential alignment in or within the macromolecule. This condition can be achieved for polymers like DNA if the fluorophore has some sort of alignment with respect to the axis of the polymer.

ACKNOWLEDGMENTS

This work was supported in part by grants from CMC PHSSUBUVGC 10641 (E.G. and M.D.), NIH, PHS 5 P41-RRO3155 (E.G. and T.H.), Ricerca Ateneo grant 2002-6059004 (M.L.B.), and a Howard Hughes undergraduate fellowship (S.G.).

REFERENCES

Aragon SR, Pecora R. 1975. Fluorescence correlation spectroscopy and Brownian rotational diffusion. Biopolymers 14:119–137.

Aragon SR, Pecora R. 1976. Fluorescence correlation spectroscopy as a probe of molecular dynamics. J Chem Phys 64:1791–1803.

Barcellona ML, Gratton E. 1996a. Torsional dynamics and orientation of DNA-DAPI complexes. Biochemistry 35:321–333.

Barcellona ML, Gratton E. 1996b. Fluorescence anisotropy of DNA/DAPI complex: torsional dynamics and geometry of the complex. Biophys J 70:2341–2351.

Berland KM, So PTC, Gratton E. 1995. Two-photon fluorescence correlation spectroscopy: method and application to the intracellular environment. Biophys J 68:694–701.

Ehrenberg M, Rigler R. 1974. Rotational Brownian motion and fluorescence intensity fluctuations. Chem Phys 4:390–401.

Elson EL, Magde D. 1974. Fluorescence correlation spectroscopy. I. Conceptual basis and theory. Biopolymers 13:1–27.

Ermak DL, McCammon JA. 1978. Brownian dynamics with hydrodynamic interactions. J Chem Phys 69:1352–1360.

Hongmei J, Vologodskii AV, Schlick T. 1997. A combined wormlike-chain and bead model for dynamic simulations of long linear DNA. J Comp Phys 136:168–179.

Inoue M, Digman M, Chang M, Breusegem SY, Halaihel N, Sorribas V, Mantulin WW, Gratton E, Barry NP, Levi M. 2004. Partitioning of NaPi cotransporter in cholesterol, sphingomyelin and glycosphingolipid enriched membrane domains modulates its activity and diffusion. J Biol Chem 279:49160–49171.

Kask P, Piksarv P, Mets U, Pooga M, Lippmaa E.1987. Fluorescence correlation spectroscopy in the nanosecond time range: Rotational diffusion of bovine carbonic anhydrase B. Eur Biophys J 14:257-261.

Kask P, Piksarv P, Pooga M, Mets U, Lippmaa E. 1988. Separation of the rotational contribution in fluorescence correlation experiments. Biophys J 55:213–220.

Magde D, Elson E, Webb WW. 1972. Thermodynamic fluctuations in a reacting system: measurement by fluorescence correlation spectroscopy. Phys Rev Lett 29:705–708.

Magde D, Elson EL, Webb WW. 1974. Fluorescence correlation spectroscopy II. An experimental realization. Biopolymers 13:29–61.

Manzini G, Barcellona ML, Quadrifoglio F. 1983. Interaction of 4′,6-diamidine-2-phenylindole (DAPI) with natural and synthetic nucleic acids. Nucleic Acids Res 11:8861–8875.

Mets U. 2001. Antibunching and rotational diffusion in FCS. In: Rigler R, Elson ES, editors. Fluorescence correlation spectroscopy, theory and applications. New York: Springer-Verlag. p 346–359.

Schurr JM, Fujimoto BS. 1988. The amplitude of local angular motions of intercalated dyes and bases in DNA. Biopolymers 27:1543–1569.

Schurr JM, Fujimoto BS, Wu P, Song L. 1992. Fluorescence studies of nucleic acids: dynamics, rigidities, and structures. In: Lakowicz JR, editor. Topics in fluorescence spectroscopy, Vol. 3. New York: Plenum Press. p 137–229.

Thompson NL. 1991. Fluorescence correlation spectroscopy. In: Lakowicz JR, editor. Topics in fluorescence spectroscopy. New York: Plenum Press. p 337–378.

Wilson WD, Tanious FA, Burton HJ, Jones RL, Fox K, Widra RL, Strekowski L. 1990. DNA sequence dependent binding modes of 4′,6-diamidino-2-phenylindole (DAPI). Biochemistry 29:8452–8461.